

# Whole body MRI of the non-human primate using a clinical 3T scanner: initial experiences

Chun-Xia Li<sup>1</sup>, Xiaodong Zhang<sup>1,2</sup>

<sup>1</sup>Yerkes Imaging Center, <sup>2</sup>Division of Neuropharmacology and Neurologic Diseases, Yerkes National Primate Research Center, Emory University, Atlanta, GA, 30329, USA

*Correspondence to:* Dr. Xiaodong Zhang, Yerkes Imaging Center, Yerkes National Primate Research Center, Emory University, 954 Gatewood Road NE, Atlanta, GA 30329, USA. Email: xzhang8@emory.edu.

**Abstract:** With the advent of parallel imaging MRI techniques, whole-body MRI is being increasingly used in clinical diagnosis. However, its application in preclinical research using large animals remains very limited. In the present study, the whole-body MRI techniques for adult macaque monkeys were explored using a conventional clinic 3T scanner. The T1, T2 anatomical images, and MR angiography of adult macaque whole bodies were illustrated. The preliminary results suggest whole-body MRI can be a robust tool to examine multiple organs of non-human primate (NHP) models from head to toe non-invasively and simultaneously using a conventional clinical setting. As NHPs are intensely used in biomedical research such as HIV/AIDS and vaccine discovery, whole body MRI techniques can have a wide range of applications in translational research using NHPs.

**Keywords:** Whole-body MRI; macaque monkey; anatomical image; high field magnet; parallel imaging

Submitted Mar 24, 2017. Accepted for publication Apr 07, 2017.

doi: 10.21037/qims.2017.04.03

**View this article at:** <http://dx.doi.org/10.21037/qims.2017.04.03>

## Introduction

Whole-body MRI allows for scanning the entire body head to toe within one scanning session, providing high-resolution multi-modality MR images such as T1 and T2 anatomical images, angiography, diffusion-weighted images of different organ systems without exposing the subject to ionizing radiation. Its clinical usage in full-body examination for disease in patients was limited previously because of the long scanning duration and poor image quality. With the advent in high field MRI and parallel imaging techniques, the image quality and scanning duration have been improved substantially (1-4), allowing for better spatial resolution and diagnostic accuracy compared to traditional PET/CT (5).

Whole body MRI techniques have been explored generally to examine the anatomical structures of multiple organs (such as neck, chest, abdomen, spine, pelvis, and extremities) and disease conditions including bleeding,

edema, lymphoma, skeletal metastases in patients (6-11), whole body inflammation (12), diabetes (13), or virtual autopsy (14). Also, it has been applied for evaluating the distribution of extensive local lesions and that of multi-organ systemic disease and lipodystrophy and fat distribution in HIV patients (15,16), and to identify inflammation and structural damages in patients with rheumatoid arthritis in order to assess the staging and treatment response during medical treatment (17). In particular, whole-body MRI and FDG PET/CT showed excellent agreement in detection of skeletal metastases of pediatric patients (18).

Non-human primates (NHPs) are our closest biological relatives and resemble most aspects of human including anatomical structures and vascular anatomy, physiology, neurology, immunology (19). NHPs are widely used in neuroscience research like stroke (20-22), aging (23,24), hippocampal lesion (25), Huntington's disease (26), drug addiction (27), developmental dysfunction (28), and infection diseases including HIV (29-35), Ebola (36) and

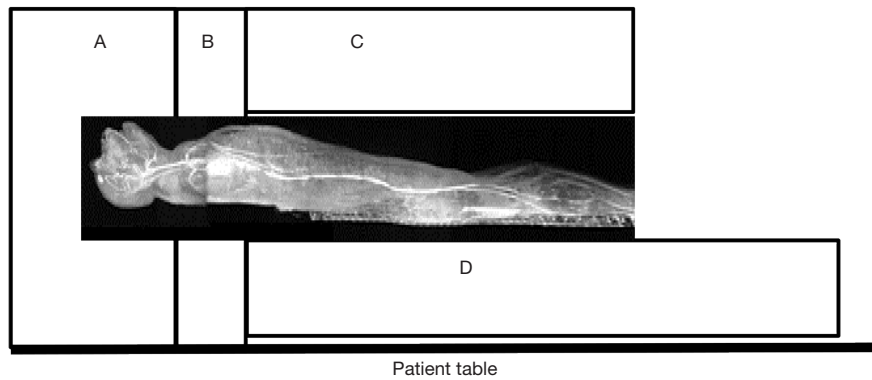


**Figure 1** Schematic drawing of the experimental settings for RF coils and a monkey in a clinical 3T MRI scanner. (A) 12-ch head coil; (B) 2-ch neck coil; (C) 4-ch FLEX coil; (D) 8-ch spinal matrix coil.

Zika virus infection (37), and vaccine discovery research (38). As seen in the studies of infectious diseases or tumors, multiple organs in the animal body can be affected during the disease evolution, and the extent and distribution of the multifocal diseases can be assessed with whole body MRI (3). However, to our knowledge, whole body MRI has not been generally utilized in large animals like NHPs. In the present study, we explored the whole-body MRI techniques for imaging the entire body of adult macaque monkeys from head to toe by using a clinical 3T MRI scanner. The preliminary results were illustrated and discussed for application in biomedical research using NHPs.

## Methods

Adult female rhesus monkeys ( $n=4$ , 7–11 years old, 8.5–10.5 kg) were initially anesthetized with Telazol (5 mg/kg, i.m.), and then switched to ~1% isoflurane mixed with 100% oxygen using an isoflurane vaporizer (Patterson Veterinary, Devens, MA, USA). The anesthetized animals were immobilized with a home-made head holder and placed in the “supine” position during MRI scan. The arms and legs were secured with belts and tapes in the scanner. Animals breathed spontaneously. Respiration rate, isoflurane concentration (end-tidal) and Et-CO<sub>2</sub> were continuously monitored with a PROCARE Monitor B40 anesthesia machine (GE Healthcare, Milwaukee, WI, USA), heart rate and O<sub>2</sub> saturation with a Nonin pulse oximeter (Nonin medical, Plymouth, MN, USA), blood pressure by a Surgivet V6000 (Smiths Medical PM, Waukesha, WI, USA), and body temperature with a Digi-Sense Temperature controller (Cole-Parmer, IL, USA), respectively. Lactated ringer’s solution was administered intravenously to prevent

dehydration during scanning. The physiological parameters were recorded and maintained in normal ranges (39).

The MRI scans were performed on a Siemens 3T TIM Trio whole body scanner (Siemens Medical Solutions USA, Medical, PA, USA) by using multiple receive-only RF array coils (12-ch head matrix coil, 2-ch neck matrix coil, 8-ch spinal matrix coil, and 4-ch FLEX large coil). The length of the body (from head to toe) of an adult macaque monkey is about 100 cm. As seen in *Figure 1*, the head and chest of the animal were covered by the head coil and neck coil. The abdomen was covered partially by the neck coil and mostly by the spinal coil under the body and the FLEX coil above the body. The legs were placed on the anterior part of the spine coil. All these coils were iPAT (integrated Parallel Acquisition Techniques) -compatible and allowed to be combined with each other to image different body parts.

The T2- weighted images (*Figure 2*) were acquired with turbo spin-echo pulse sequences and scanning parameters: TR =7,880 ms, TE =114 ms, data matrix =288×384 and FOV =203 mm × 905 mm, slice thickness =4.0 mm (composed images). The T1-weighted images (*Figure 3*) were acquired using turbo spin-echo sequence with TR =260 ms, TE =2.5 ms, BW =268 Hz, data matrix =160×256, FOV =195 mm × 250 mm, slice thickness =4.0 mm. 3D time-of-flight (TOF) MR angiogram (MRA) pulse sequence (flip angle =18°; TE =3.6 ms; TR =20 ms) was used to acquire the vascular images, spatial resolution: 0.25×0.25×2.00 mm<sup>3</sup> for head and neck (*Figure 4A,B*), 0.51×0.51×4.40 mm<sup>3</sup> for lower part of the body (*Figure 4C,D*). The composing software (Siemens) was utilized for composing of MR images from different table positions in order to create whole body anatomy images. All images were processed with a Siemens work station installed with

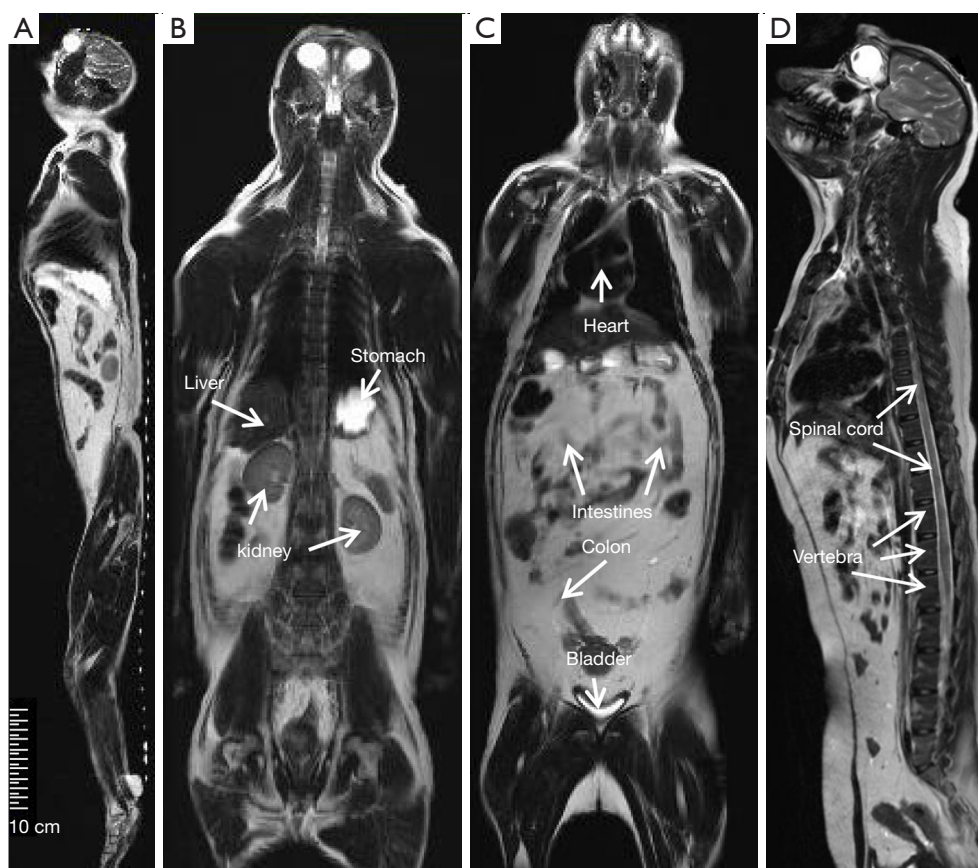


**Figure 2** Composed T2-weighted anatomical images of an adult macaque. (A) Sagittal image, from head to toe; (B,C,D) body images to show important organs such as liver, kidney, stomach (coronal, B); heart, intestines, colon and bladder (coronal, C); and spine (sagittal, D). Artifacts in (A) are from heating pad.

Siemens Sygno MRI data processing software.

All procedures followed the protocols approved by the Institutional Animal Care and Use Committee (IACUC) of Emory University in accordance with the NIH Guide for Care and Use of Laboratory Animals.

## Results

The T2-weighted anatomical images of the entire body of adult macaques were acquired. One sagittal slice of the body from head to toe is shown in *Figure 2A*, in which the anatomical images of brain, chest, abdomen, muscle, knee, and toe are demonstrated with one composed image. Also, important organs such as liver, kidney, bladder, heart, intestines and colon and spine are specifically illustrated (*Figure 2B,C,D*). The T1-weighted anatomical images (sagittal and axial) of a macaque monkey abdomen are illustrated in *Figure 3*. MR Angiographies of the whole body

head to toe, specific regions for brain and neck are also shown (*Figure 4*). As seen in the illustrated images, the brain and neck angiography, structural anatomy of liver, kidneys, spine cord, and intestine of an adult monkey can be clearly identified with whole body MRI using a conventional clinical setting.

## Discussion

These preliminary results indicate the whole-body MRI techniques can be a robust approach to simultaneously examine multiple organs of the entire body of adult macaque monkeys non-invasively by using the conventional clinical settings. In addition, multiple modalities including T1 and T2 weighted imaging, MRA, and other techniques like DWI, can be conducted in the same subject and in the same scanning session to provide complementary information for screening or evaluation of the disease staging and treatment

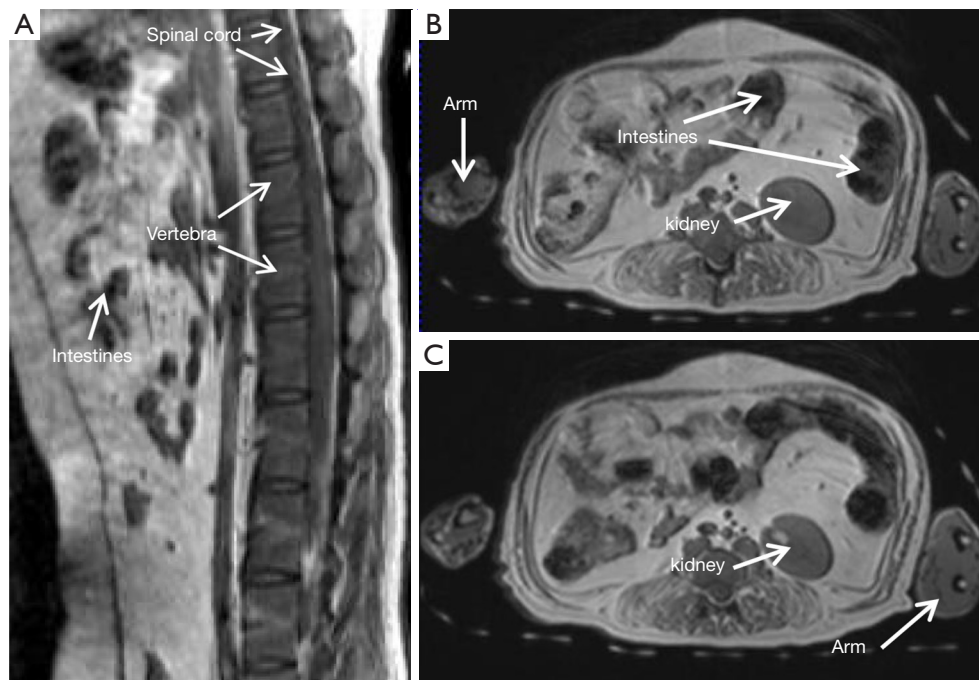


**Figure 3** T1-weighted anatomical images of an adult macaque abdomen to show important organs such as spine, intestines (sagittal A); kidney, intestines, arms (coronal, B and C).

response. In particular, as NHPs are anesthetized during scanning, the scan duration can be extended for several hours to allow for specific and detailed examination from whole body screening to region-specific imaging of multiple organs, which cannot be conducted readily in clinical patients. Therefore, NHP models can be further exploited to assess and optimize the clinical protocols in whole-body MRI examinations of pediatric patients.

Compared to other species, NHPs resemble most aspects of human, and are excellent animal models in biomedical research including infection diseases such as HIV/AIDS (38). Antiretroviral therapy (ART) is generally used for HIV patients. However, there is no cure for HIV disease (40), and HIV/AIDS is still spreading worldwide. Currently, NHP models are intensively used for finding a safe and effective cure for HIV/AIDS patients (41).

HIV infects the cells of the immune system, resulting in an immune-deficient state and severe pathology across multiple organ systems in the body. CD4<sup>+</sup> T cells are a primary target of HIV and CD4 cell depletion is a major factor in the pathogenesis of HIV infection (42). Also, CD8<sup>+</sup> T cells play a critical role in controlling HIV viremia and reducing overall numbers of HIV-infected cells in

approaches to eradicate HIV(43,44). Due to their roles in the process of the adaptive immune system, tracking these T cells *in vivo* will play a critical role in drug discovery and modern vaccine development (45,46).

*In vivo* molecular imaging has emerged as a promising means for immune cell tracking to study immune cell proliferation, apoptosis and interaction at the microscopic and macroscopic level with living subjects (47). Currently there are two different labeling strategies for immune cell tracking: (I) direct labeling by using probes that are internalized by immune cells; (II) indirect labeling with genetic modification. Among the several imaging techniques including CT, PET, SPECT, MRI, optical imaging, and ultrasound, MRI can provide high spatial and temporal resolution with the use of iron oxide- particles and <sup>19</sup>F-based probes for image-guided immune cell delivery and visualization of immune cell homing and engraftment, inflammation, cell physiology and gene expression (48). Available MRI techniques include using Gadolinium-based T1 contrast agent, superparamagnetic iron oxide nanoparticles (SPIONs) based T2 contrast agent, and molecular probes containing <sup>19</sup>F or inducing chemical exchange saturation transfer (CEST) signals. Cell tracking

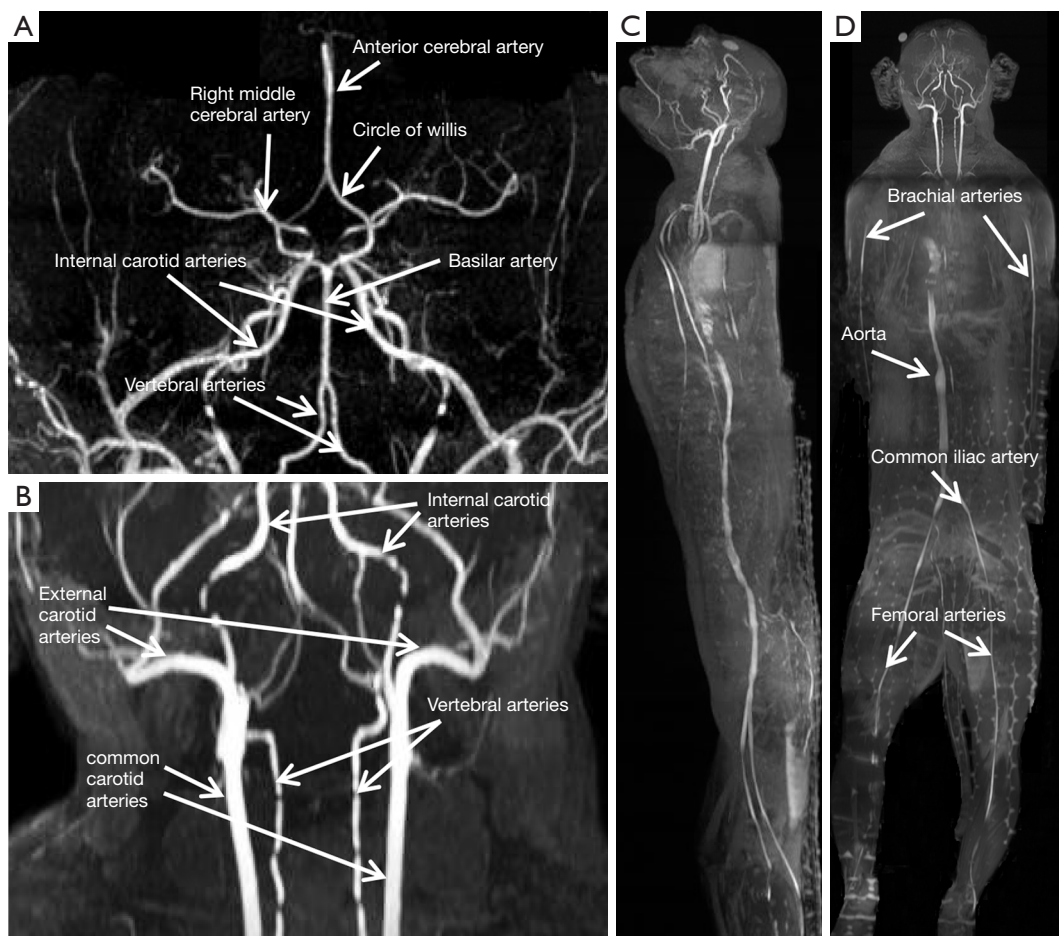


**Figure 4** Regional MR angiography images (A: brain, B: neck) and composed vascular images of sagittal (C) and coronal (D) planes of an adult macaque from head to toe.

with SPIONs has been used in cell-based therapy (49,50). It has been explored previously to image immune cell (such as CD4 T+ cells, CD8 T+ cells, and Mac1+ cells) location and homing in the central nervous system of mice with superparamagnetic antibodies (51).

Molecular imaging has been successfully applied to visualize simian immunodeficiency virus (SIV)-infected cells in the body of rodent models of HIV (52). Like human, lymph nodes are located throughout the whole body of a macaque monkey. Therefore, we believe the whole body MRI based molecular imaging can be exploited as an effective tool in disease diagnosis and evaluation of brain and other organs of macaque models of HIV/AIDS.

The site and source of virus replication cannot be identified by using traditional examinations with blood, CSF, and biopsies. Recently, an *in vivo* viral imaging method

has shown its effectiveness in detecting whole-body SIV replication by using  $^{64}\text{Cu}$ -labeled SIV Gp120-specific antibody with whole-body PET (53). The signals are detected in the gastrointestinal, respiratory tract, lymphoid tissues and reproductive organs of viremic monkeys, demonstrating its wide application in HIV/AIDS research and drug and vaccine development. As a technical limitation, the signal cannot be seen in brain. It is very important to identify the sites and sources of virus replication in the entire body in approaches to eradicate HIV as they may serve as viral reservoirs. Nanoparticles have very small size and can go anywhere in the body. Therefore, the molecular imaging with whole body MRI can provide complementary information about the infection progress in the whole body including brain and other organs.

Whole-body MRI has emerged to be a promising

means for the screening, diagnosis, staging and response assessment in pediatric cancer patients due to its superior contrast resolution and tissue characterization (7,54). However, MRI in young children is usually performed under sedation or general anesthesia for motion control in clinic (55,56). Preclinical studies suggest anesthetics may have neurotoxic effects on the developing brain (57). There is a strong concern to sedate young children during MRI scanning. NHPs are important models in cancer therapy (58-61). Therefore, whole body MRI techniques can be intensively explored with the NHP models to optimize and improve its detection capacity in pediatric oncology.

Certainly, the whole body MR imaging approaches are not limited to what we discussed above and can be further facilitated with the advent of new techniques and are capable to be translated into other research fields such as pharmaceutical and neuroscience studies using NHP models. Also, this study is aimed to demonstrate the potential and capacities for imaging the entire body of large animals from head to toe using different modalities on a conventional clinic scanner. As a limitation, the spatial resolution and image contrast of the demonstrated whole body images in this study were not fully-optimized. but the imaging quality in the entire body or specific regions or organs can be further improved when experimental parameters are specifically optimized or using customer-built coils and/or performing more averages with respiratory-gating for anesthetized monkeys.

## Conclusions

The preliminary results suggest the whole-body MRI techniques can be a robust approach to examine the brain and other multiple body organs of macaque monkeys non-invasively and simultaneously. In particular, its application in HIV/AIDS research can be further exploited using immune cell tracking techniques to examine the whole body including brain and other organs. Furthermore, whole body MRI of NHPs can be intensively explored for other preclinical studies such as cancer research and imaging protocol development and optimization in clinical diagnosis of pediatric oncology.

## Acknowledgements

The authors are grateful to Sudeep Patel, Ruth Connelly, and Doty Kempf (DVM) for assistance in data acquisition and animal handling, and technical support from Siemens.

*Funding:* The project was funded by the National Center for Research Resources (P51RR000165) and is currently supported by the Office of Research Infrastructure Programs (OD P51OD011132).

## Footnote

*Conflicts of Interest:* The authors have no conflicts of interest to declare.

## References

1. Machann J, Schlemmer HP, Schick F. Technical challenges and opportunities of whole-body magnetic resonance imaging at 3T. *Phys Med* 2008;24:63-70.
2. Chavhan GB, Babyn PS. Whole-body MR imaging in children: principles, technique, current applications, and future directions. *Radiographics* 2011;31:1757-72.
3. Eutsler EP, Khanna G. Whole-body magnetic resonance imaging in children: technique and clinical applications. *Pediatr Radiol* 2016;46:858-72.
4. Hernandez M, Semelka R, Júnior J, Bamrungchart S, Dale B, Stallings C. Whole-body MRI: comprehensive evaluation on a 48-channel 3T MRI system in less than 40 minutes. Preliminary results. *Radiol Bras* 2012;45:319-25.
5. Schmidt GP, Schoenberg SO, Schmid R, Stahl R, Tiling R, Becker CR, Reiser MF, Baur-Melnyk A. Screening for bone metastases: whole-body MRI using a 32-channel system versus dual-modality PET-CT. *Eur Radiol* 2007;17:939-49.
6. McBride KA, Ballinger ML, Schlub TE, Young MA, Tattersall MH, Kirk J, Eeles R, Killick E, Walker LG, Shanley S, Thomas DM, Mitchell G. Psychosocial morbidity in TP53 mutation carriers: is whole-body cancer screening beneficial? *Fam Cancer* 2017.
7. Guimaraes MD, Noschang J, Teixeira SR, Santos MK, Lederman HM, Tostes V, Kundra V, Oliveira AD, Hochegger B, Marchiori E. Whole-body MRI in pediatric patients with cancer. *Cancer Imaging* 2017;17:6.
8. Latifoltojar A, Hall-Craggs M, Rabin N, Popat R, Bainbridge A, Dikaios N, Sokolska M, Rismani A, D'Sa S, Punwani S, Yong K. Whole body magnetic resonance imaging in newly diagnosed multiple myeloma: early changes in lesional signal fat fraction predict disease response. *Br J Haematol* 2017;176:222-33.
9. van Ufford HM, Kwee TC, Beek FJ, van Leeuwen MS, Takahara T, Fijnheer R, Nievelstein RA, de Klerk JM. Newly diagnosed lymphoma: initial results with whole-

- body T1-weighted, STIR, and diffusion-weighted MRI compared with 18F-FDG PET/CT. *AJR Am J Roentgenol* 2011;196:662-9.
10. Lauenstein TC, Goehde SC, Herborn CU, Goyen M, Oberhoff C, Debatin JF, Ruehm SG, Barkhausen J. Whole-body MR imaging: evaluation of patients for metastases. *Radiology* 2004;233:139-48.
  11. Schmidt GP, Haug AR, Schoenberg SO, Reiser MF. Whole-body MRI and PET-CT in the management of cancer patients. *Eur Radiol* 2006;16:1216-25.
  12. Axelsen MB, Eshed I, Ostergaard M, Hetland ML, Moller JM, Jensen DV, Krintel SB, Hansen MS, Terslev L, Klarlund M, Poggenborg RP, Balding L, Pedersen SJ. Monitoring total-body inflammation and damage in joints and entheses: the first follow-up study of whole-body magnetic resonance imaging in rheumatoid arthritis. *Scand J Rheumatol* 2017;1-10.
  13. Bamberg F, Hetterich H, Rospleszcz S, Lorbeer R, Auweter SD, Schlett CL, Schafnitzel A, Bayerl C, Schindler A, Saam T, Muller-Peltzer K, Sommer W, Zitzelsberger T, Machann J, Ingrisch M, Selder S, Rathmann W, Heier M, Linkohr B, Meisinger C, Weber C, Ertl-Wagner B, Massberg S, Reiser MF, Peters A. Subclinical Disease Burden as Assessed by Whole-Body MRI in Subjects With Prediabetes, Subjects With Diabetes, and Normal Control Subjects From the General Population: The KORA-MRI Study. *Diabetes* 2017;66:158-69.
  14. Andronikou S, Kemp ML, Meiring M. Whole-Body MRI Virtual Autopsy Using Diffusion-weighted Imaging With Background Suppression (DWIBS) at 3 T in a Child Succumbing to Chordoma. *J Pediatr Hematol Oncol* 2017;39:133-6.
  15. Engelson ES, Kotler DP, Tan Y, Agin D, Wang J, Pierson RN Jr., Heymsfield SB. Fat distribution in HIV-infected patients reporting truncal enlargement quantified by whole-body magnetic resonance imaging. *Am J Clin Nutr* 1999;69:1162-9.
  16. Garcia AI, Milinkovic A, Tomas X, Rios J, Perez I, Vidal-Sicart S, Pomes J, Del Amo M, Mallolas J. MRI signal changes of the bone marrow in HIV-infected patients with lipodystrophy: correlation with clinical parameters. *Skeletal Radiol* 2011;40:1295-301.
  17. Axelsen MB, Eshed I, Duer-Jensen A, Moller JM, Pedersen SJ, Ostergaard M. Whole-body MRI assessment of disease activity and structural damage in rheumatoid arthritis: first step towards an MRI joint count. *Rheumatology (Oxford)* 2014;53:845-53.
  18. Kumar J, Seith A, Kumar A, Sharma R, Bakhshi S, Kumar R, Agarwala S. Whole-body MR imaging with the use of parallel imaging for detection of skeletal metastases in pediatric patients with small-cell neoplasms: comparison with skeletal scintigraphy and FDG PET/CT. *Pediatr Radiol* 2008;38:953-62.
  19. Uno H. Age-related pathology and biosenescent markers in captive rhesus macaques. *Age (Omaha)* 1997;20:1-13.
  20. Zhang X, Tong F, Li CX, Yan Y, Kempf D, Nair G, Wang S, Muly EC, Zola S, Howell L. Temporal evolution of ischemic lesions in nonhuman primates: a diffusion and perfusion MRI study. *PLoS One* 2015;10:e0117290.
  21. Cook DJ, Teves L, Tymianski M. Treatment of stroke with a PSD-95 inhibitor in the gyrencephalic primate brain. *Nature* 2012;483:213-U112.
  22. Zhang X, Tong F, Li CX, Yan Y, Nair G, Nagaoka T, Tanaka Y, Zola S, Howell L. A fast multiparameter MRI approach for acute stroke assessment on a 3T clinical scanner: preliminary results in a non-human primate model with transient ischemic occlusion. *Quant Imaging Med Surg* 2014;4:112-22.
  23. Chen X, Errangi B, Li L, Glasser MF, Westlye LT, Fjell AM, Walhovd KB, Hu X, Herndon JG, Preuss TM, Rilling JK. Brain aging in humans, chimpanzees (*Pan troglodytes*), and rhesus macaques (*Macaca mulatta*): magnetic resonance imaging studies of macro- and microstructural changes. *Neurobiol Aging* 2013;34:2248-60.
  24. Yan Y, Li L, Preuss TM, Hu X, Herndon JG, Zhang X. In vivo evaluation of optic nerve aging in adult rhesus monkey by diffusion tensor imaging. *Quantitative imaging in medicine and surgery* 2014;4:43-9.
  25. Meng Y, Payne C, Li L, Hu X, Zhang X, Bachevalier J. Alterations of hippocampal projections in adult macaques with neonatal hippocampal lesions: A Diffusion Tensor Imaging study. *Neuroimage* 2014;102P2:828-37.
  26. Chan AW, Jiang J, Chen Y, Li C, Prucha MS, Hu Y, Chi T, Moran S, Rahim T, Li S, Li X, Zola SM, Testa CM, Mao H, Villalba R, Smith Y, Zhang X, Bachevalier J. Progressive cognitive deficit, motor impairment and striatal pathology in a transgenic Huntington disease monkey model from infancy to adulthood. *PLoS One* 2015;10:e0122335.
  27. Murnane KS, Howell LL. Neuroimaging and drug taking in primates. *Psychopharmacology (Berl)* 2011;216:153-71.
  28. Sanchez MM. The impact of early adverse care on HPA axis development: nonhuman primate models. *Hormones and Behavior* 2006;50:623-31.
  29. Li C, Zhang X, Komery A, Li Y, Novembre FJ, Herndon JG. Longitudinal diffusion tensor imaging and perfusion

- MRI investigation in a macaque model of neuro-AIDS: a preliminary study. *Neuroimage* 2011;58:286-92.
30. Li CX, Zhang X, Komery A, Li Y, Mao H, Herndon JG, Novembre FJ. Longitudinal cerebral metabolic changes in pig-tailed macaques infected with the neurovirulent virus SIV<sub>smmFGb</sub>. *J Neurovirol* 2014;20:612-9.
  31. Micci L, McGary CS, Paiardini M. Animal models in HIV cure research. *J Virus Erad* 2015;1:17-22.
  32. Williams K, Lackner A, Mallard J. Non-human primate models of SIV infection and CNS neuropathology. *Curr Opin Virol* 2016;19:92-8.
  33. Ponte R, Mehraj V, Ghali P, Couedel-Courteille A, Cheynier R, Routy JP. Reversing Gut Damage in HIV Infection: Using Non-Human Primate Models to Instruct Clinical Research. *EBioMedicine* 2016;4:40-9.
  34. Rahmberg AR, Rajakumar PA, Billingsley JM, Johnson RP. Dynamic Modulation of Expression of Lentiviral Restriction Factors in Primary CD4+ T Cells following Simian Immunodeficiency Virus Infection. *J Virol* 2017;91.
  35. Chahroudi A, Silvestri G. What pediatric nonprogressors and natural SIV hosts teach us about HIV. *Sci Transl Med* 2016;8:358fs16.
  36. Ohimain EL. Recent advances in the development of vaccines for Ebola virus disease. *Virus Res* 2016;211:174-85.
  37. Morrison TE, Diamond MS. Animal Models of Zika Virus Infection, Pathogenesis, and Immunity. *J Virol* 2017;91. doi: 10.1128/JVI.00009-17.
  38. Rivera-Hernandez T, Carnathan DG, Moyle PM, Toth I, West NP, Young PR, Silvestri G, Walker MJ. The contribution of non-human primate models to the development of human vaccines. *Discov Med* 2014;18:313-22.
  39. Li CX, Patel S, Auerbach EJ, Zhang X. Dose-dependent effect of isoflurane on regional cerebral blood flow in anesthetized macaque monkeys. *Neurosci Lett* 2013;541:58-62.
  40. Margolis DM, Koup RA, Ferrari G. HIV antibodies for treatment of HIV infection. *Immunol Rev* 2017;275:313-23.
  41. Policicchio BB, Pandrea I, Apetrei C. Animal Models for HIV Cure Research. *Front Immunol* 2016;7:12.
  42. Zunich KM, Lane HC. Immunologic abnormalities in HIV infection. *Hematol Oncol Clin North Am* 1991;5:215-28.
  43. Mylvaganam GH, Rios D, Abdelaal HM, Iyer S, Tharp G, Mavinger M, Hicks S, Chahroudi A, Ahmed R, Bosinger SE, Williams IR, Skinner PJ, Velu V, Amara RR. Dynamics of SIV-specific CXCR5+ CD8 T cells during chronic SIV infection. *Proc Natl Acad Sci U S A* 2017;114:1976-81.
  44. Takata H, Buranapraditkun S, Kessing C, Fletcher JL, Muir R, Tardif V, Cartwright P, Vandergeeten C, Bakeman W, Nichols CN, Pinyakorn S, Hansasuta P, Kroon E, Chalermchai T, O'Connell R, Kim J, Phanuphak N, Robb ML, Michael NL, Chomont N, Haddad EK, Ananworanich J, Trautmann L. Delayed differentiation of potent effector CD8+ T cells reducing viremia and reservoir seeding in acute HIV infection. *Sci Transl Med* 2017;9. doi: 10.1126/scitranslmed.aag1809.
  45. Baumjohann D, Ansel KM. Tracking early T follicular helper cell differentiation in vivo. *Methods Mol Biol* 2015;1291:27-38.
  46. Iyer SS, Gangadhara S, Victor B, Gomez R, Basu R, Hong JJ, Labranche C, Montefiori DC, Villinger F, Moss B, Amara RR. Codelivery of Envelope Protein in Alum with MVA Vaccine Induces CXCR3-Biased CXCR5+ and CXCR5- CD4 T Cell Responses in Rhesus Macaques. *J Immunol* 2015;195:994-1005.
  47. Youn H, Hong KJ. In vivo non invasive molecular imaging for immune cell tracking in small animals. *Immune Netw* 2012;12:223-9.
  48. Ahrens ET, Bulte JW. Tracking immune cells in vivo using magnetic resonance imaging. *Nat Rev Immunol* 2013;13:755-63.
  49. Ngen EJ, Wang L, Kato Y, Krishnamachary B, Zhu W, Gandhi N, Smith B, Armour M, Wong J, Gabrielson K, Artemov D. Imaging transplanted stem cells in real time using an MRI dual-contrast method. *Sci Rep* 2015;5:13628.
  50. Jasmin, de Souza GT, Louzada RA, Rosado-de-Castro PH, Mendez-Otero R, Campos de Carvalho AC. Tracking stem cells with superparamagnetic iron oxide nanoparticles: perspectives and considerations. *Int J Nanomedicine* 2017;12:779-93.
  51. Pirko I, Johnson A, Ciric B, Gamez J, Macura SI, Pease LR, Rodriguez M. In vivo magnetic resonance imaging of immune cells in the central nervous system with superparamagnetic antibodies. *FASEB J* 2004;18:179-82.
  52. Song J, Cai Z, White AG, Jin T, Wang X, Kadayakkara D, Anderson CJ, Ambrose Z, Young WB. Visualization and quantification of simian immunodeficiency virus-infected cells using non-invasive molecular imaging. *The Journal of general virology* 2015;96:3131-42.
  53. Santangelo PJ, Rogers KA, Zurla C, Blanchard EL, Gumber S, Strait K, Connor-Stroud F, Schuster DM, Amancha PK, Hong JJ, Byrareddy SN, Hoxie JA, Vidakovic B, Ansari AA, Hunter E, Villinger F. Whole-body immunPET reveals active SIV dynamics in viremic



- and antiretroviral therapy-treated macaques. *Nat Methods* 2015;12:427-32.
54. Smith EA, Dillman JR. Current role of body MRI in pediatric oncology. *Pediatr Radiol* 2016;46:873-80.
55. Santangelo PJ, Rogers KA, Zurla C, Blanchard EL, Gumber S, Strait K, Connor-Stroud F, Schuster DM, Amancha PK, Hong JJ, Byrareddy SN, Hoxie JA, Vidakovic B, Ansari AA, Hunter E, Villinger F. Pediatric neuroimaging in early childhood and infancy: challenges and practical guidelines. *Ann N Y Acad Sci* 2012;1252:43-50.
56. Jaimes C, Gee MS. Strategies to minimize sedation in pediatric body magnetic resonance imaging. *Pediatr Radiol* 2016;46:916-27.
57. Mintz CD, Wagner M, Loepke AW. Preclinical research into the effects of anesthetics on the developing brain: promises and pitfalls. *J Neurosurg Anesthesiol* 2012;24:362-7.
58. Xia HJ, Chen CS. Progress of non-human primate animal models of cancers. *Dongwuxue Yanjiu* 2011;32:70-80.
59. Lapin BA, Yakovleva LA. Spontaneous and experimental malignancies in non-human primates. *J Med Primatol* 2014;43:100-10.
60. Daniels TR, Martinez-Maza O, Penichet ML. Animal models for IgE-mediated cancer immunotherapy. *Cancer Immunol Immunother* 2012;61:1535-46.
61. Lu KH, Yates MS, Mok SC. The monkey, the hen, and the mouse: models to advance ovarian cancer chemoprevention. *Cancer Prev Res (Phila)* 2009;2:773-5.

**Cite this article as:** Li CX, Zhang X. Whole body MRI of the non-human primate using a clinical 3T scanner: initial experiences. *Quant Imaging Med Surg* 17;7(2):267-275. doi: 10.21037/qims.2017.04.03